ORNL-TM-3961

Contract No. W-7405-eng-26

Neutron Physics Division

CALCULATIONS OF NEUTRON FLUX SPECTRA INDUCED IN THE EARTH'S ATMOSPHERE BY GALACTIC COSMIC RAYS*

T. W. Armstrong
K. C. Chandler†
J. Barish†

Note:
Research partially funded by
NATIONAL AERONAUTICS AND SPACE ADMINISTRATION
under Order H-38280A

*Submitted for journal publication.
†Mathematics Division.

OCTOBER 1972

OAK RIDGE NATIONAL LABORATORY
Oak Ridge, Tennessee, 37830
operated by
UNION CARBIDE CORPORATION
for the
U. S. ATOMIC ENERGY COMMISSION

Abstract

Calculations have been carried out to determine the neutron flux induced in the earth's atmosphere by galactic protons and alpha particles at solar minimum for a geomagnetic latitude of 42°N. Neutron flux spectra in the energy range from $\sim 10^{-8}$ to $\sim 10^{5}$ MeV at various depths in the atmosphere were calculated using Monte Carlo and discrete ordinates methods, and various comparisons with experimental data are presented. The magnitude and shape of the calculated neutron-leakage spectrum at the particular latitude considered support the theory that the cosmic-ray-albedo-neutron-decay (CRAND) meachanism is the source of the protons and electrons trapped in the Van Allen belts.

INTRODUCTION

Some of the neutrons produced in the earth's atmosphere by cosmic-ray bombardment escape and subsequently decay within the magnetosphere into protons and electrons. It was initially proposed by Singer [1958] that this cosmic-ray-albedo-neutron-decay (CRAND) mechanism is the source of the protons and electrons trapped in the Van Allen radiation belts. Previous efforts (e.g., Dragt *et al.* [1966]; Hess and Killeen [1966]) to test this hypothesis have shown serious discrepancies between measured trapped-proton intensities and the intensities predicted by the CRAND theory. For example, Dragt *et al.* [1966] found the theoretical intensity at 55 MeV to be a factor of 50 too small. However, these predicted intensities have been based on neutron albedo spectra obtained from rather approximate calculations [Lingenfelter, 1963], especially for that portion of the albedo spectra $\gtrsim$ 10 MeV, and at least part of the discrepancy may be ascribed to uncertainties in the magnitude of the neutron albedo spectra used in predicting the proton intensities. Since the time of the Lingenfelter calculations, there has been considerable progress in the development of calculational methods for estimating the nucleon-meson cascade induced in matter by high-energy hadrons (e.g., Armstrong *et al.* [1972]), and therefore the present calculations were undertaken in an effort to better define the magnitude of the neutron albedo by using a calculational method that requires fewer approximations than previously used.

In the present work, the Monte Carlo code HETC [Chandler and Armstrong, 1972] was used to compute the production and transport of protons, charged pions, and neutrons (> 12 MeV) due to protons and alpha particles incident on the top of the atmosphere. The neutron production ≤ 12 MeV from the HETC

BLANK PAGE

calculation was used as input to the discrete ordinates code ANISN [Engle, 1967] to obtain the low-energy (≤ 12 MeV) portion of the neutron spectra. The basic input for this method of calculation is the proton and alpha-particle spectra incident at the top of the atmosphere. This differs from most methods used previously to calculate the neutron albedo (e.g., Lingenfelter [1963]; Newkirk [1963]; Hess *et al.* [1961]) in which the low-energy (≲ 10 MeV) neutron production was estimated from rather sparse experimental data, and only the low-energy (≲ 10 MeV) transport calculations were carried out in detail. Thus, the magnitude of the neutron fluxes computed here are based on experimental data for the galactic proton and alpha-particle spectra, whereas the normalization for the neutron fluxes from previous calculations has been determined from measurements of the low-energy neutrons in the atmosphere.

In the next section the calculational details are given. The calculations have been carried out for a geomagnetic latitude of 42°N and for solar-minimum proton and alpha-particle spectra. The calculations for incident alpha particles are more approximate than those for incident protons because in its present form the code HETC cannot treat alpha-particle-nucleus interactions, and therefore a rather crude model had to be used to obtain the description of the particles produced by alpha-particle interactions.

In the last section the results are presented and discussed. Although the primary interest here is the neutron spectrum at the top of the atmosphere, the neutron spectra at various depths in the atmosphere have also been calculated and are compared with experimental data to provide a check on the accuracy of the calculational method for present purposes.

CALCULATIONAL DETAILS

Calculational Method: Incident Protons

The Monte Carlo code HETC [Chandler and Armstrong, 1972] was used to compute the transport of protons, charged pions, primary alpha particles, and neutrons > 12 MeV, and the discrete ordinates code ANISN [Engle, 1967] was used for the low-energy (≤ 12 MeV) neutron transport. Since the standard version of HETC cannot transport alpha particles, the calculational method used for incident protons is discussed first, and the modifications to the code that were made to treat incident alpha particles in an approximate manner are discussed later.

Monte Carlo techniques, in conjunction with theoretical nuclear-interaction models, are used in the high-energy code HETC to determine in detail the nucleon-meson cascade. The methods used in HETC for treating various physical processes are described in detail elsewhere [Armstrong *et al.*, 1972], so only a brief description of those aspects of the code pertinent to the present problem will be described here. HETC takes into account charged-particle energy loss due to atomic ionization and excitation, nonelastic nucleon-nucleus and pion-nucleus collisions, elastic neutron-nucleus collisions, and pion decay in flight and at rest. For nucleons above 3.5 GeV and pions above 2.5 GeV, nuclear interactions are treated using the intranuclear-cascade-extrapolation-evaporation model of Gabriel *et al.* [1970]. This model uses the particle-production data, obtained from an intranuclear-cascade calculation for intermediate-energy (~ 3 GeV) nucleon-nucleus and pion-nucleus collisions, together with energy, angle, and multiplicity-scaling relations, which are consistent with the sparse experimental data for high-energy collisions, to estimate the particle production for higher energy

($\gtrsim$ 3 GeV) collisions. For nucleons between 12 MeV and 3.5 GeV and pions between 1.8 MeV and 2.5 GeV, nuclear interactions are treated using the intranuclear-cascade-evaporation model of Bertini and Guthrie [1971]. At each nuclear interaction that occurs during the Monte Carlo simulation of the nucleon-meson cascade, a calculation is performed to determine the energy, direction, and number of the interaction products, and the recoil energy, charge, and mass of the residual nucleus. The particles produced in nuclear interactions may be protons, neutrons, charged pions, and neutral pions from the intranuclear cascade and protons, neutrons, deuterons, tritons, ^{3}He's, and alpha particles from the evaporation. The produced neutral pions are assumed to decay immediately into two photons, and these photons, as well as all photons produced in nuclear interactions, are neglected. The heavy particles ($A > 1$) produced by evaporation are assumed to slow down and come to rest at their point of origin without undergoing nuclear interaction. Neutrons and protons above 12 MeV and charged pions above 1.8 MeV are followed until they eventually escape from the atmosphere, undergo nuclear absorption, or, in the case of charged pions, decay. Protons that slow down to 12 MeV or are produced below 12 MeV and charged pions that slow down to 1.8 MeV or are produced below 1.8 MeV are assumed to come to rest without undergoing nuclear interaction. Because of the relatively low density of the atmosphere, it is much more probable that negatively charged pions that come to rest will decay rather than undergo nuclear capture, so both positive and negatively charged pions reaching 1.8 MeV were assumed to decay. Muons from pion decay were neglected. The treatment of neutrons produced below 12 MeV is discussed later.

The accuracy of the code HETC for predicting the characteristics of nucleon-meson cascades has been checked for source-particle energies up to ~ 30 GeV, and, in general, good agreement with experimental data has been found [Armstrong *et al.*, 1972]. Also, there is considerable indirect evidence that the code is reasonably accurate at energies much higher than 30 GeV (e.g., Armstrong *et al.* [1972]; Armstrong and Alsmiller [1971]).

Since the nuclear-interaction models used in HETC are inapplicable at very low energies, the neutron production ≤ 12 MeV computed by HETC was used as input to the discrete-ordinates code ANISN [Engle, 1967] to obtain the low-energy neutron transport. The neutron cross sections for the ANISN calculations were obtained from the ENDF/B cross section library [ENDF/B, 1970] and put in multigroup form by using the code XLACS [Greene *et al.*, 1972]. The ANISN calculations were made using 57 spatial intervals, $S_{16}P_3$ angular quadrature, and 32 energy groups, with upscattering allowed in the lowest 13 energy groups. Upscattering allows neutrons to gain as well as lose energy in elastic collisions with nuclei, and it is needed to properly predict the shape of the neutron spectrum at very low (near thermal) energies.

Calculational Method: Incident Alpha Particles

It was necessary to resort to a very approximate method to treat incident alpha particles. The position in the atmosphere at which an alpha particle experienced its first nuclear collision was determined using a mean free path based on the cross section $\sigma_i = \pi(r_\alpha + r_i)^2$, where r_α and r_i are effective radii for the alpha particle and the struck nucleus (nitrogen and oxygen), respectively, and are given by $r = 1.17 \times 10^{-13} A^{1/3}$ cm [Webber, 1967]. The energy of the alpha particle at the collision site was obtained using the stopping-power formula for protons, with an approximate density-effect correction [Armstrong and Alsmiller, 1970] and scaling relations (e.g., Barkas and Berger [1964]). To obtain the energy and direction of the collision products, a very approximate model [Gabriel, Santoro, and Alsmiller, 1971] was used in which it is assumed that the nucleons of the alpha particle enter the nucleus separately and independently except for their relative spatial locations when they enter the nucleus with each nucleon having a kinetic energy equal to one-quarter of the difference between the kinetic energy and the binding energy of the alpha particle. From the products produced by all four of the incident nucleons and from the energy and momentum conservation, the charge, mass, and excitation energy of the residual nucleus were determined, and an evaporation calculation for the collision was then made. These assumptions allow the products from alpha-particle collisions to be computed using the standard collision models contained in HETC. The cascade initiated by the alpha-particle collision products was calculated in exactly the same manner as described previously for incident protons.

Other Calculational Details

The calculations have been made for an isotropic flux of galactic protons and alpha particles incident on an infinite slab of atmosphere (79 atom % N, 21% O) 1033 g/cm^2 in thickness, and the ground was represented by a layer of SiO_2 ~ 500 g/cm^2 in thickness with a density of 1.8 g/cm^3. The density variation of the atmosphere [U.S. Standard Atmosphere, 1962] was taken into account since the pion decay probability per unit distance is density-dependent.

The temperature variation with altitude was taken into account in the generation of the low-energy (< 12 MeV) neutron cross sections for the ANISN code. The following values [Hess, Canfield, and Lingenfelter, 1961] for the temperature in various depth intervals (measured from the top of the atmosphere) were used:

0 - 235 g/cm^2	:	219°K
235 - 485 g/cm^2	:	234°K
485 - 710 g/cm^2	:	260°K
710 - 1033 g/cm^2	:	280°K
> 1033 g/cm^2	:	300°K

The proton and alpha-particle spectra presented in the review article by McDonald [1969] were used. These spectra are based on several balloon and satellite measurements made near the solar minimum in 1965 with a power law in energy extrapolation at high ($\gtrsim$ 10 GeV/nucleon) energies.

The calculations have been made for a vertical cutoff rigidity of 4.6 GV, which corresponds to a vertical cutoff energy of 3.8 GeV for protons and 6.3 GeV for alpha particles, and (for a dipole field) a geomagnetic latitude of $\lambda = 42°$. Incident protons in the energy range from 3.8 GeV to 200 GeV and incident alpha particles in the energy range from 6.3 GeV to 800 GeV were considered in the calculations. The geomagnetic cutoff at non-vertical angles was taken into account although at the latitude considered here the cutoff is rather sharp; i.e., no particles with energies less than the vertical cutoff energy penetrate the magnetic field and essentially all particles with energies greater than the vertical cutoff are transmitted. The details of the procedure used in selecting source-particle energies and directions with the effect of the geomagnetic cutoff included are discussed in Appendix A.

RESULTS

Neutron Flux Spectra vs Depth

The calculated omnidirectional (over 4π) neutron-flux spectra at various depths in the atmosphere are shown in Figs. 1 and 2. At depths of 0 g/cm^2 (top of atmosphere), 200 g/cm^2, and 1033 g/cm^2 (air-ground interface), calculated neutron spectra due only to incident protons are also shown to indicate the contribution of incident alpha particles to the neutron spectra at these depths. Error bars are shown for those portions of the spectra (> 12 MeV) calculated using the Monte Carlo methods. The error bars shown in these and subsequent figures correspond to estimated statistical errors of one standard deviation. Statistical fluctuations are also associated with the results < 12 MeV since the neutron source distribution for the discrete ordinates calculation is obtained by the Monte Carlo methods. The statistical error < 12 MeV is estimated to lie generally between 5 and 25%.

The neutron spectrum calculated by Lingenfelter [1963] at 0 g/cm^2 is also shown in Fig. 1. This spectrum is referred to as the neutron flux spectrum in the Lingenfelter paper, but, according to commonly accepted nomenclature (e.g., Beckurts and Wirtz [1964]), the quantity actually calculated was the neutron current spectrum [Lingenfelter, 1972]. The neutron current spectrum at 0 g/cm^2 is also available from the present calculations and is shown in Fig. 1. The neutron spectrum calculated here is in good agreement with that calculated by Lingenfelter at low ($\leqslant$ 10 MeV) energies, but the spectrum calculated here is considerably higher for energies $\geqslant$ 10 MeV. However, from the nature of the calculational method used by Lingenfelter, his spectrum is expected to be very approximate at energies $\geqslant$ 10 MeV.

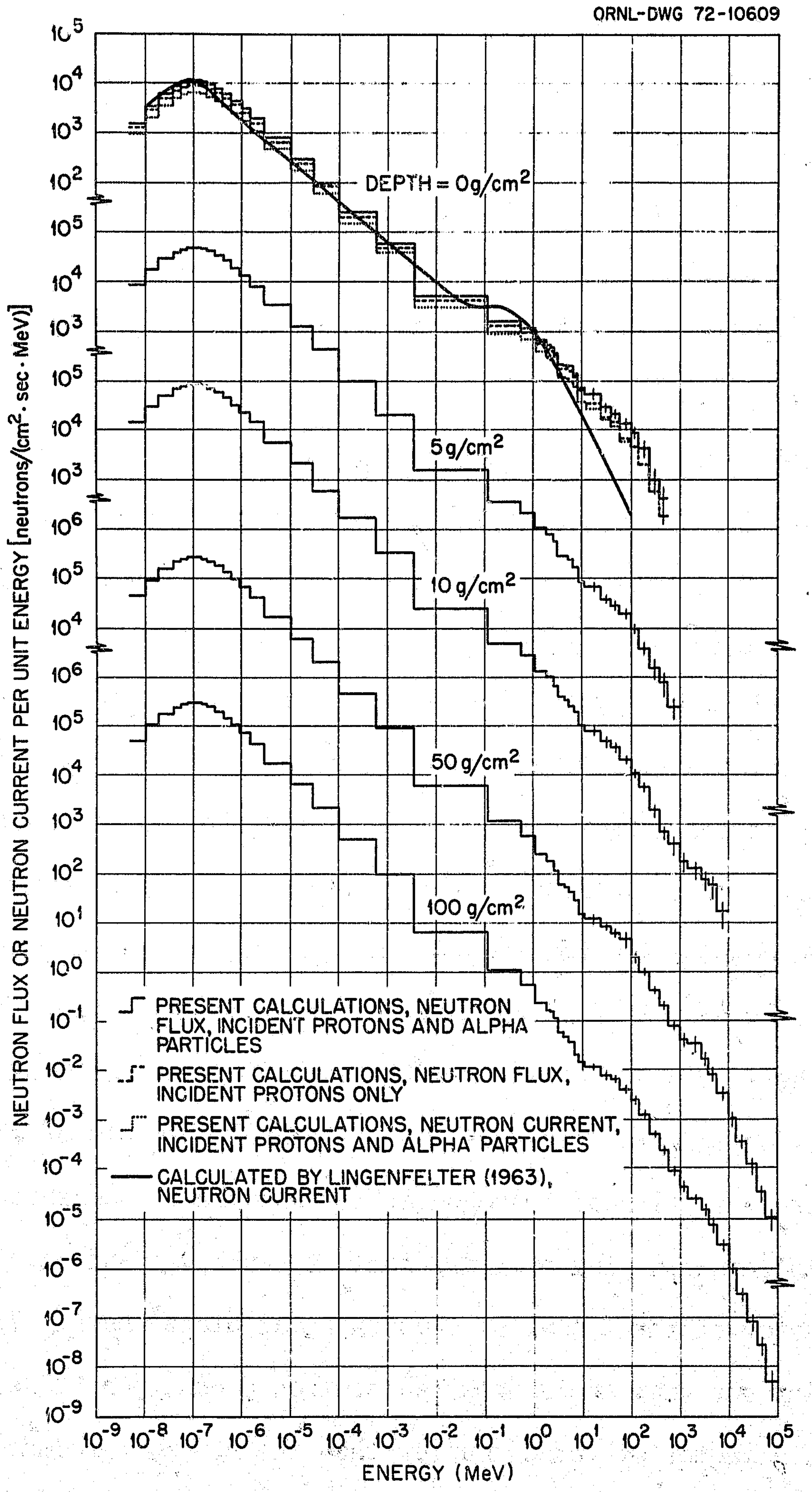

Fig. 1. Neutron spectra at various depths from the top of the atmosphere. Solar minimum, $\lambda = 42^{o}N$.

The neutron-flux spectra measured in 1956-1957 by Hess *et al.* [1959] at depths of 200 and 1033 g/cm^2 are also shown in Fig. 2. The measured and calculated spectra differ somewhat at low energies, especially in the thermal-energy region, but are in quite good agreement at high energies. The accuracy of the measured spectra at very low energies ($\leqslant 4 \times 10^{-8}$ MeV) is estimated by Hess *et al.* [1959] to be about a factor of two.

Neutron Flux vs Depth

The depth dependence of the neutron flux in several energy ranges is shown in Fig. 3. The calculated fluxes are compared with the measurements of Boella *et al.* [1965] ($\lambda = 42^{o}$N, 1963) in the energy range from thermal to 20 MeV and with the measurements of Holt *et al.* [1966] ($\lambda = 42^{o}$N, 1964) in the 1- to 10-MeV region. The statistical error (one standard deviation) for the calculated results is generally less than 20%, with the greatest uncertainty at the larger depths. The fluxes show considerable variation near the air-ground interface. This variation is, of course, dependent upon the assumed composition for the ground. In the present calculations, SiO_2 with a density of 1.8 g/cm^3 was used to simulate dry soil. The addition of water to the soil would have a significant effect on the low-energy neutron flux (see, for example, Yamashita *et al.* [1966]) because of the large absorption cross section of hydrogen at low energies. Yamashita *et al.* [1966] measured the neutron flux over dry soil at sea level and obtained a flux about a factor of three smaller than that calculated here. Yamashita *et al.* [1966] point out that their measured neutron production at sea level is also about a factor of three smaller than the neutron production predicted from the data of Hess *et al.* [1959, 1961] and Newkirk [1963]. O'Brien [1971] calculated the depth dependence of the neutron flux in the atmosphere using an essentially analytical propagation theory and a phenomenological

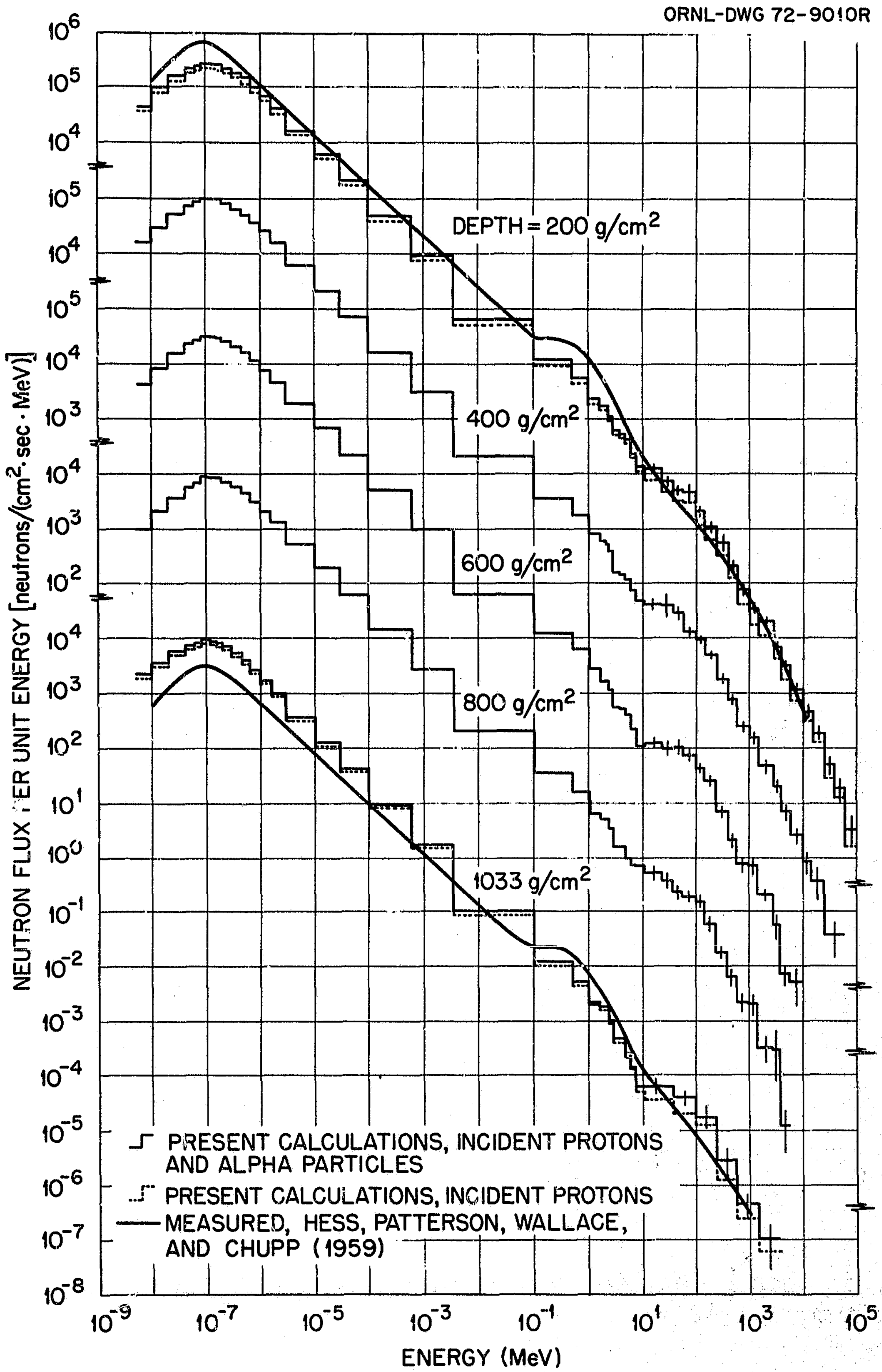

Fig. 2. Neutron spectra at various depths from the top of the atmosphere. Solar minimum, $\lambda = 42^{\circ}N$.

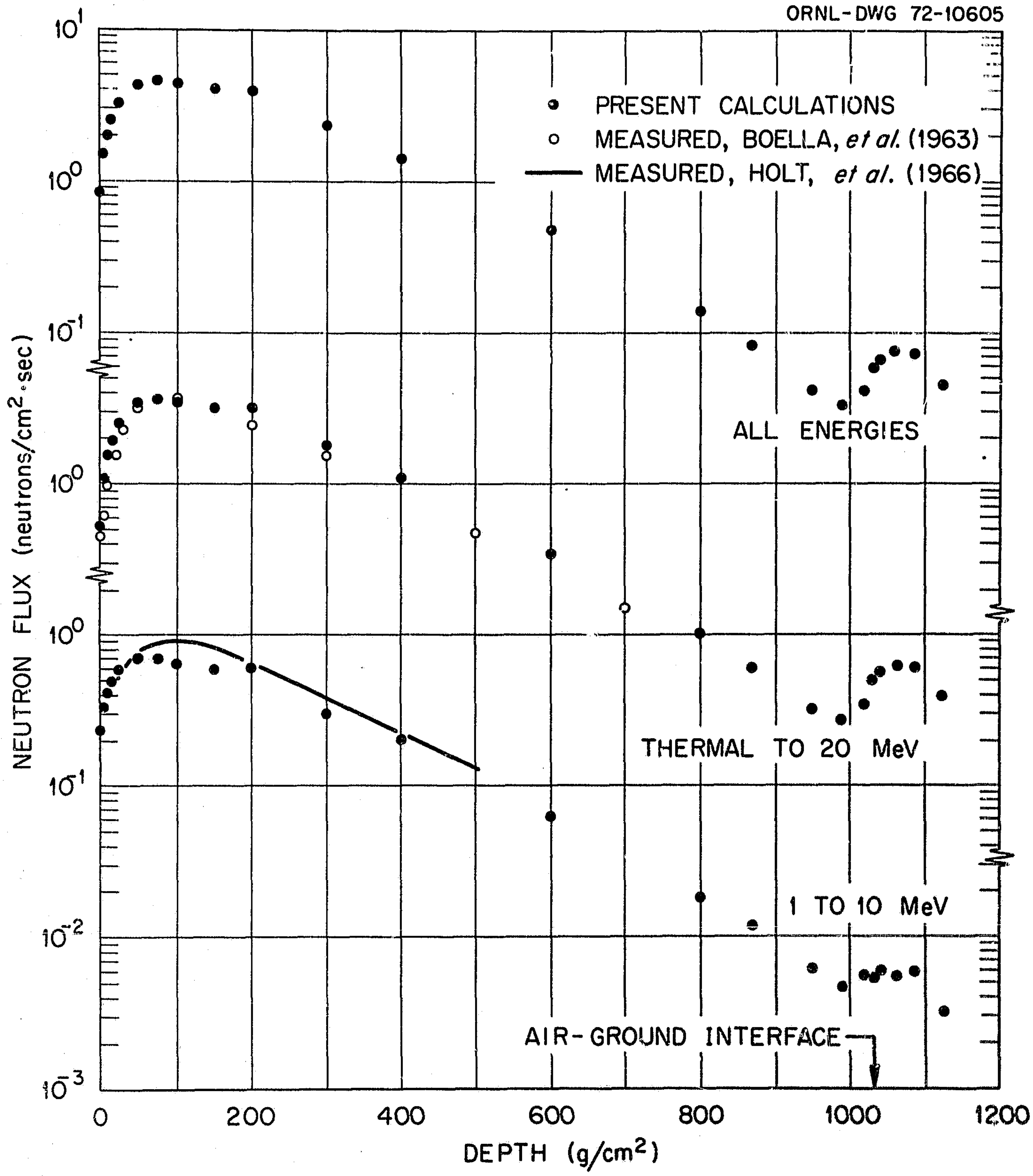

Fig. 3. Depth dependence of neutron flux in various energy intervals. Solar minimum, $\lambda = 42^{o}N$.

model for hadron-nucleus collisions. His calculations, which neglect the ground, predict neutron fluxes near sea level substantially lower than the fluxes calculated here.

A comparison of the spatial dependence of the neutron flux in the 1- to 10-MeV range near the top of the atmosphere at $\lambda \approx 42^{\circ}$N is shown in Fig. 4. The fluxes from the present calculations with and without incident alpha particles included are shown, which indicate that for this particular latitude and energy and spatial regions incident alpha particles contribute $\approx$ 17%. The range of values shown in Fig. 4 from Haymes [1964] represent approximately the spread in the data obtained from four balloon flights. These measurements were made in 1963 with a detector sensitive to neutrons in the 1- to 14-MeV range. (According to the energy dependence of the flux measured by Haymes [1964], the neutron flux in the 1- to 14-MeV range is approximately 10% higher than the 1- to 10-MeV flux.) The results of the diffusion-theory calculations of Lingenfelter [1963] and the discrete ordinates calculations of Newkirk [1963] shown in Fig. 4 were taken from the paper of Haymes [1964]. (Lingenfelter's results in this case are in terms of flux, not current [Lingenfelter, 1972].) Newkirk's calculated results for $\lambda = 57^{\circ}$N and (presumably) 1961 were converted to $\lambda = 42^{\circ}$N by Haymes [1964] using the latitude dependence calculated by Lingenfelter [1963]. The measurements of Holt *et al.* [1966] were made at $\lambda = 42^{\circ}$N during the latter part of 1964 using a detector sensitive to neutrons in the 1- to 10-MeV range. Thus, the results shown in Fig. 4 are for common conditions with the exceptions that the Haymes data are for 1 to 14 MeV instead of 1 to 10 MeV and the Haymes and Newkirk data are not at solar minimum. According to the measurements of Merker *et al.* [1969], the 1- to 10-MeV neutron flux at $\lambda = 42^{\circ}$N can vary by $\approx$ 20% during a solar cycle.

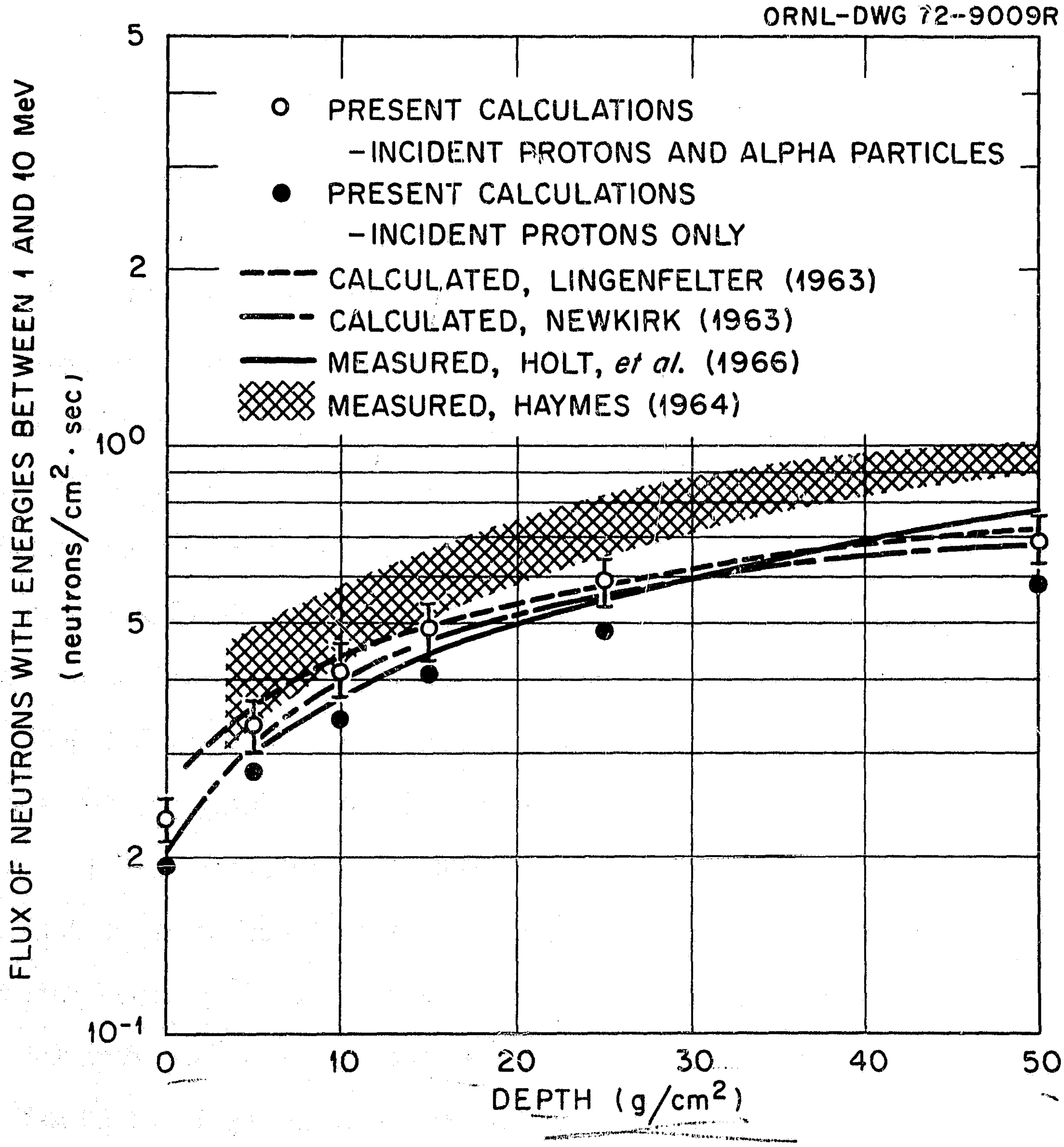

Fig. 4. Depth dependence of the flux of neutrons with energies between 1 and 10 MeV near the top of the atmosphere.

Haymes [1964] and Holt *et al.* [1966] extrapolated their data near the top of the atmosphere to obtain the flux at 0 g/cm^2, and these extrapolated fluxes are given in Table 1, together with calculated values for the flux at 0 g/cm^2. Thus, at $\lambda = 42^{\circ}$N both the calculations and measurements give quite consistent results for the neutron flux in the 1- to 10-MeV region at the top of the atmosphere.

Neutron Spectrum Near the Top of the Atmosphere

In Fig. 5 portions of the calculated flux spectra at depths of 0 and 5 g/cm^2 are shown and compared with the calculations of Lingenfelter [1963], the measurements of Holt *et al.* [1966] and Preszler *et al.* [1972], and an approximate estimate made by Freden and White [1962]. At 5 g/cm^2 both the calculated and measured [Preszler *et al.*, 1972] spectra are for only the upward moving neutrons, i.e., the flux per unit energy due to neutrons having directions between $\theta = 0^{\circ}$ and $\theta = 90^{\circ}$ with respect to the zenith direction.

As pointed out earlier, the Lingenfelter energy spectrum (solar minimum, $\lambda = 40^{\circ}$N) is for the neutron current, not the neutron flux. The Holt *et al.* [1966] spectrum is from data taken in late 1964 at $\lambda = 42^{\circ}$N and has an $E^{-1.0}$ energy dependence. The measurements of Preszler *et al.* [1972] were made in 1971 at $\lambda = 40^{\circ}$N. Freden and White [1962] estimated the neutron albedo spectrum needed to produce trapped proton spectra in agreement with proton measurements made in the radiation belt at L = 1.30 and B = 0.200. Their prediction used the CRAND theory of injection and took into account proton losses in the atmosphere due to ionization and nuclear collisions but did not take into account the injection coefficient. Preszler *et al.* [1972] multiplied the Freden and White [1962] spectrum by seven to take into account the injection coefficient calculated by Dragt, Austin, and White

TABLE 1

1- to 10-MeV Neutron Flux at 0 g/cm^2
($\lambda \approx 42^{\circ}N$)

Source	Flux (neutrons/$cm^2 \cdot sec$)
Present calculations	0.23 ± 0.02
Calculated, Lingenfelter[a]	0.26
Calculated, Newkirk[a]	0.20
Measured, Holt *et al.* [1966]	0.26
Measured, Haymes [1964]	0.24 ± 0.02

a. From the Haymes [1964] paper.

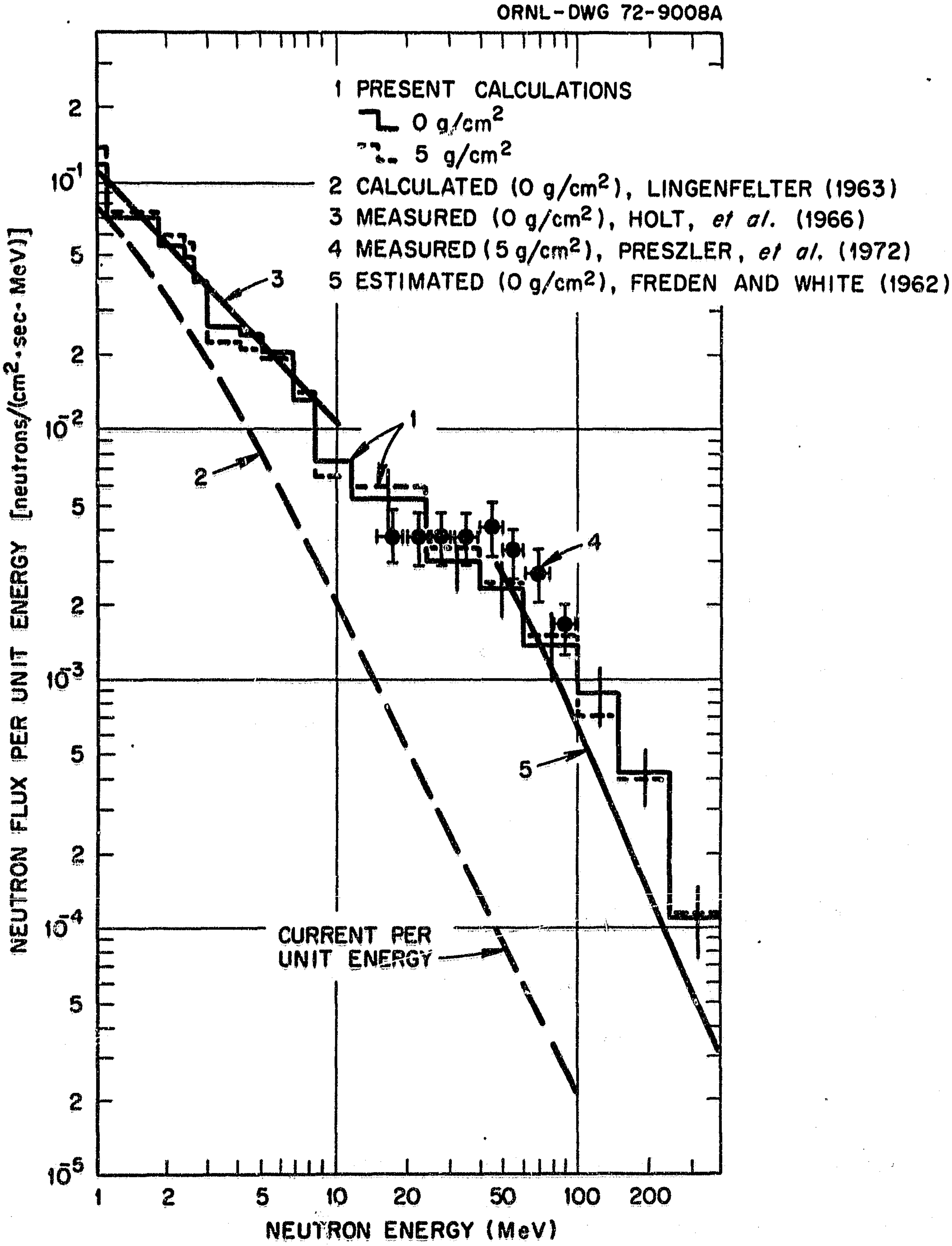

Fig. 5. Neutron spectra near the top of the atmosphere. At 5 g/cm^2, both the calculated and measured spectra are for upward-moving neutrons.

[1966], and it is the Freden and White spectrum as modified by Preszler *et al.* that is shown in Fig. 5. Leavitt [1972] recently measured the neutron albedo spectrum in the energy range from ≈ 50 to ≈ 150 MeV, and, although final analysis of the data has not yet been completed, Leavitt's preliminary data indicate a spectrum considerably lower in magnitude than that measured by Preszler *et al.* [1972]. Zobel *et al.* [1972] measured the neutron-flux spectrum between about 3 and 60 MeV at 9 g/cm^2. Their measured spectrum over most of the energy range is lower by a factor of two or more than the spectrum at 10 g/cm^2 calculated here (Fig. 1).

A comparison at a depth of 5 g/cm^2 of the omnidirectional flux spectrum and the calculated and measured [Preszler *et al.* 1972] flux spectra due to upward moving neutrons is shown in Fig. 6. White *et al.* [1972] reanalyzed the data of Preszler *et al.* to obtain the upward moving current spectrum, and Fig. 6 shows the measured and calculated current spectra due to upward moving neutrons and the calculated omnidirectional current spectrum. The spectra shown in Fig. 6 are defined as:

$$\begin{aligned}\phi_{4\pi}(E) &= \text{the omnidirectional flux spectrum}\\ &= \text{the angular flux spectrum integrated over } 4\pi \text{ solid angle}\\ &= \int_0^{2\pi} d\psi \int_{-1}^{+1} d\mu\ \phi(E,\psi,\mu)\end{aligned}$$

$$\begin{aligned}\phi_{2\pi}(E) &= \text{the upward moving flux spectrum}\\ &= \text{the angular flux spectrum integrated over } 2\pi \text{ solid angle}\\ &\quad \text{about the zenith direction}\\ &= \int_0^{2\pi} d\psi \int_0^{1} d\mu\ \phi(E,\psi,\mu)\ ;\end{aligned}$$

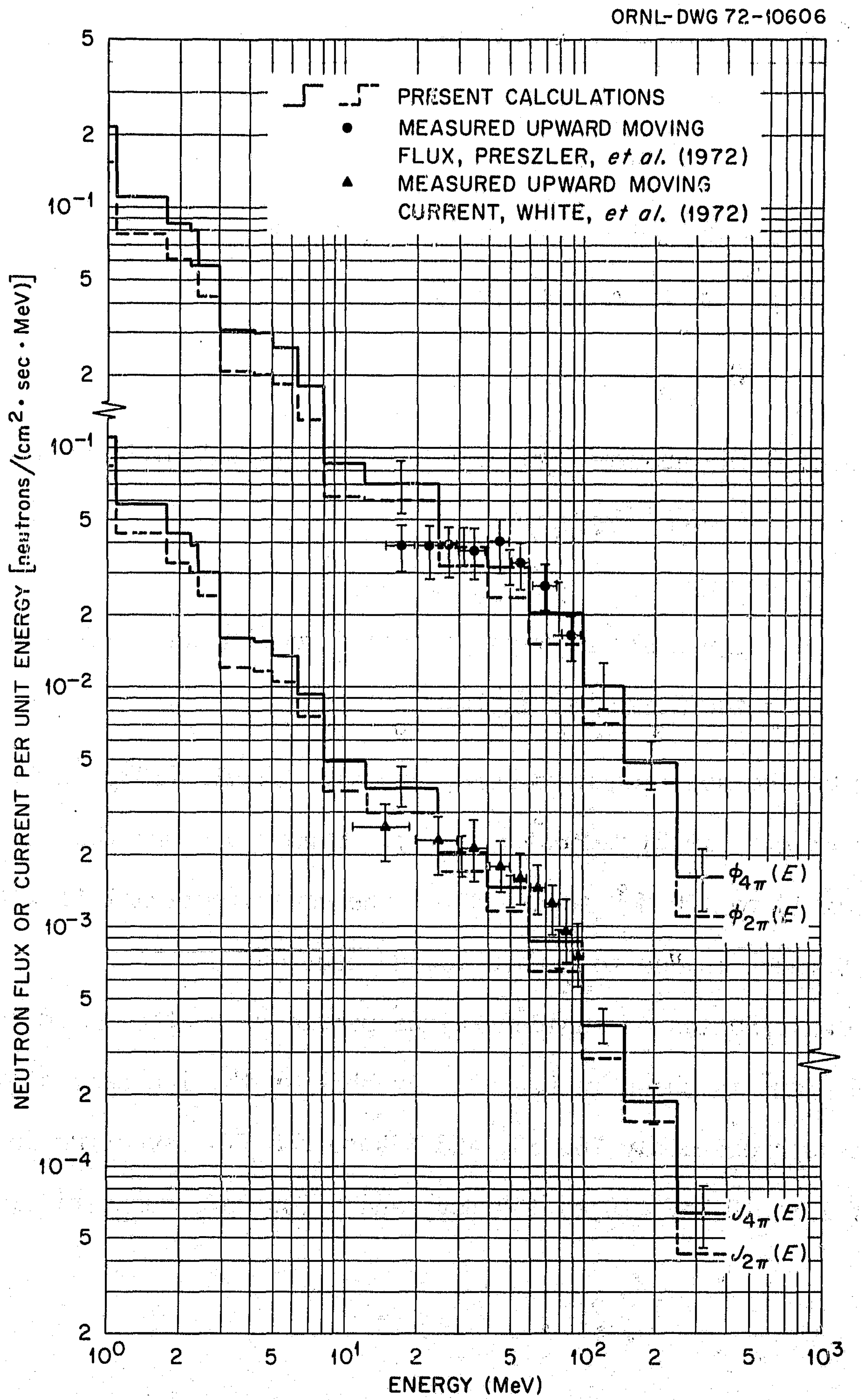

Fig. 6. Neutron flux and current spectra at 5 g/cm^2. The measured upward moving flux and current correspond to $\phi_{2\pi}(E)$ and $J_{2\pi}(E)$, respectively.

$J_{4\pi}(E)$ = the omnidirectional current spectrum

$$= \int_0^{2\pi} d\psi \int_{-1}^{+1} d\mu \ |\mu| \ \phi(E,\psi,\mu) \ ;$$

$J_{2\pi}(E)$ = the upward moving current spectrum

$$= \int_0^{2\pi} d\psi \int_0^{1} d\mu \ \mu \ \phi(E,\psi,\mu) \ ;$$

where

$\phi(E,\psi,\mu)$ = the neutron flux per unit energy and solid angle at 5 g/cm^2 depth,

$\mu = \cos\theta$,

θ = the angle between neutron direction and zenith angle,

ψ = the azimuthal angle.

According to the notation used here, Preszler *et al.* [1972] measured $\phi_{2\pi}(E)$ and White *et al.* [1972] measured $J_{2\pi}(E)$. Figure 6 shows that in the energy region from 10 to 100 MeV about 80% of the omnidirectional flux (and current) at 5 g/cm^2 is due to upward moving neutrons.

The contribution of incident alpha particles to the omnidirectional flux at 5 g/cm^2 is shown in Fig. 7. At this depth, incident alpha particles contribute approximately 20, 35, and 45% to the flux spectrum in the energy ranges of 1 to 10 MeV, 10 to 100 MeV, and > 100 MeV, respectively.

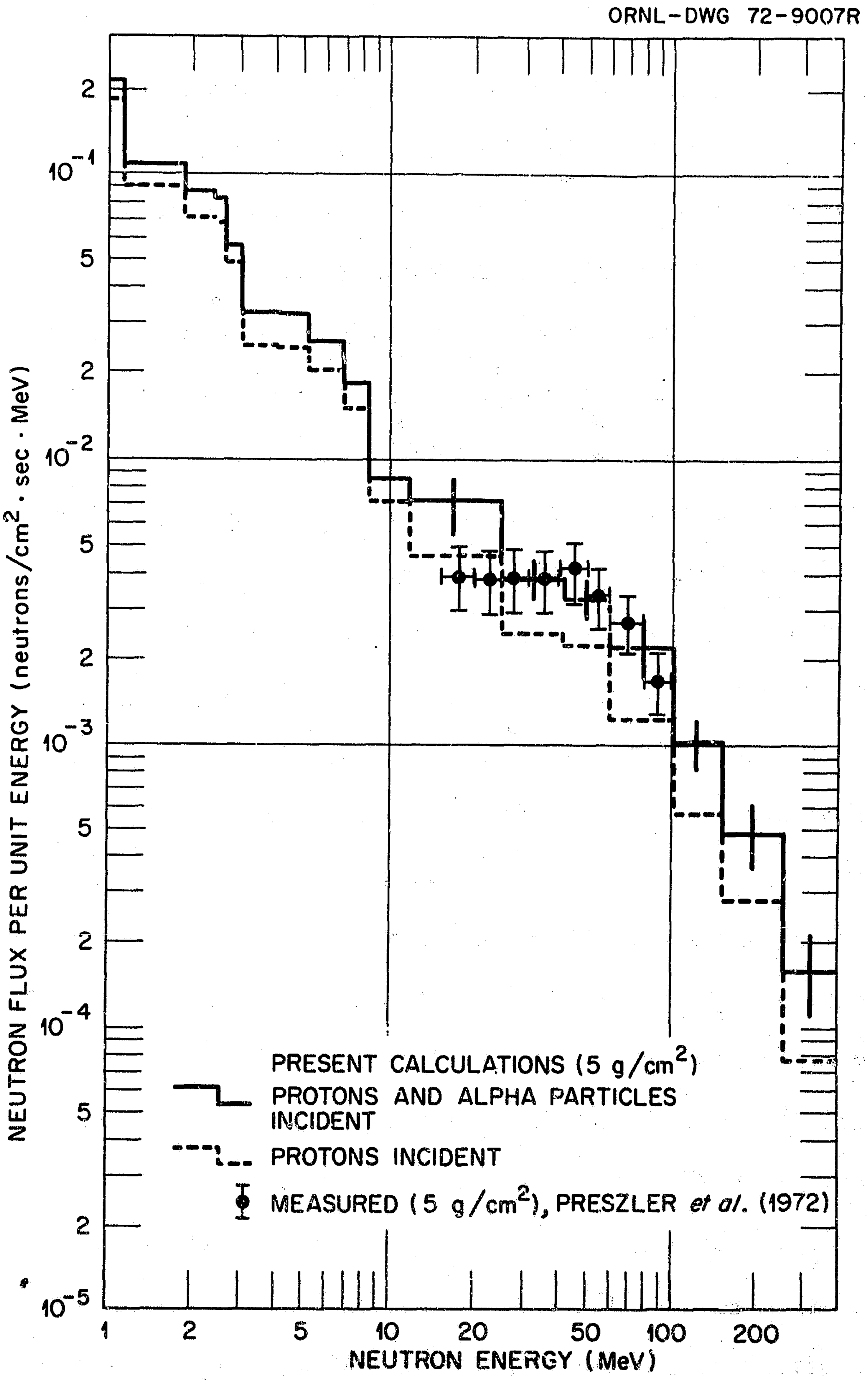

Fig. 7. Contribution of incident alpha particles to the neutron flux at 5 g/cm^2.

DISCUSSION

Dragt, Austin, and White [1966] used the neutron albedo spectrum calculated by Lingenfelter [1963] (shown in Fig. 5) and the theory of cosmic-ray-albedo-neutron-decay (CRAND) injection to arrive at a theoretical estimate of the proton intensity in the earth's radiation belt. The theoretical value of the proton flux at 55 MeV was found to be a factor of 50 smaller than the proton flux measured by Filz and Holeman [1965]. Major uncertainties in the theoretical estimate were the albedo neutron flux and the mean atmospheric densities encountered by trapped protons, and Dragt, Austin, and White [1966] concluded that agreement between theory and experiment could be obtained only if the ratio of the albedo-neutron flux to the atmospheric density used in the calculations was increased by a factor of 50. Figure 5 shows that the neutron leakage flux at 55 MeV calculated here is about a factor of 33 higher than the neutron leakage predicted by Lingenfelter [1963]. At a depth of 5 g/cm^2, the measurements of Preszler *et al.* [1972] and the present calculations give fluxes at 55 MeV that are factors of about 45 and 35, respectively, higher than the Lingenfelter [1963] curve. Thus, both the present calculations and the recent experimental data of Preszler *et al.* [1972] indicate that the CRAND theory is capable of correctly predicting the high-energy ($\geq$ 20 MeV) proton intensities observed in the inner zone of the Van Allen radiation belt. Neutron leakage spectra at other geomagnetic latitudes are needed to allow revised injection [Dragt, Austin, and White, 1966] and diffusion [Farley, Tomassian, and Walt, 1970] calculations to be made to obtain additional tests of the CRAND theory.

APPENDIX A

SELECTION OF SOURCE-PARTICLE ENERGIES AND DIRECTIONS AND THE INFLUENCE OF THE GEOMAGNETIC FIELD

First we consider the straightforward case of selecting energies and directions from the galactic proton or alpha-particle spectrum without regard to geomagnetic-field effects or any importance sampling. The omnidirectional (over 4π) flux spectrum outside the geomagnetic field, $\phi_o(E)$, is considered known and assumed to be isotropic; i.e.,

$$\phi(E,\bar{\Omega}) = \frac{\phi_o(E)}{4\pi} ,$$

where $\bar{\Omega}$ is a unit vector along the direction of travel of the particle. The corresponding current spectrum incident toward the earth is

$$\begin{aligned} J(E,\bar{\Omega}) &= \phi(E,\bar{\Omega})\ \bar{\Omega}\bullet\bar{n} \text{ , when } \bar{\Omega}\bullet\bar{n} \geq 0 \text{ ,} \\ &= 0 \text{ , otherwise,} \end{aligned}$$

where $\bar{n}$ is the unit vector normal to, and directed into, the atmosphere. The current spectrum can be written in terms of the properly normalized source distribution, $S(E,\bar{\Omega})$, for selecting energies and directions as

$$J(E,\bar{\Omega}) = \frac{\Phi}{4} S(E,\bar{\Omega}) ,$$

where

$$\begin{aligned} \frac{\Phi}{4} &= \int_{E_{min}}^{E_{max}} dE \int_{2\pi} d\bar{\Omega}\ J(E,\bar{\Omega}) \\ &= \frac{1}{4} \int_{E_{min}}^{E_{max}} dE\ \phi_o(E) \end{aligned}$$

$$S(E,\bar{\Omega}) = J(E,\bar{\Omega})/[\int_{E_{min}}^{E_{max}} \int_{2\pi} d\bar{\Omega}\ J(E,\bar{\Omega})] ,$$

and E_{min} and E_{max} define the source-particle energy range being considered. By rewriting $S(E,\bar{\Omega})$,

$$J(E,\psi,\mu)\ dE\ d\psi\ d\mu = \frac{\Phi}{4}\left[\frac{\phi_o(E)}{\Phi}\ dE\right]\left|\frac{d\psi}{2\pi}\right|\ [2\mu\ d\mu]$$

$$= W_o\ p_1(E)\ dE\ p_2(\psi)\ d\psi\ p_3(\mu)\ d\mu \quad ,$$

where

ψ = the azimuthal angle,

$\theta = \cos^{-1}\mu = \cos^{-1}(\bar{\Omega}\cdot\bar{n})$ = zenith angle,

$W_o = \Phi/4$,

$p_1(E) = \phi_o(E)/\Phi$,

$p_2(\psi) = 1/2\pi$,

$p_3(\mu) = 2\mu$.

Source-particle energies and directions can then be realized by selecting E, ψ, and μ according to the probability density functions (p.d.f.'s) p_1, p_2, and p_3, and giving each source particle the statistical weight W_o.

Because the flux spectrum $\phi_o(E)$ decreases very rapidly with increasing energy, it is almost imperative that some importance sampling be used in the energy selection to obtain adequate statistics for the effects produced by high-energy source particles. Therefore, the following biased p.d.f. for E was used instead of $p_1(E)$:

$$p_1^*(E)\ dE = p_i^!\ p''(E|i)\ dE$$

$$= p_i^!\ \frac{dE}{(E_{i+1}-E_i)} \quad ,$$

where

p_i' = the fraction of source particles to be selected in energy group i,

$p''(E|i)$ = the p.d.f. for selecting E given that E lies within energy group i,

and

$$\sum_i \int_{E_i}^{E_{i+1}} p_i^*(E)\, dE = 1 \; .$$

Values for p_i' were assigned to give greater emphasis to the high-energy portion of the spectrum than specified by $p_1(E)$. The statistical weight for a source particle selected within energy group i then becomes

$$W = W_o\, p_1(E)/p_i^*(E)$$

$$= \frac{\phi(E)}{4} (E_{i+1} - E_i)/p_i' \; .$$

Using the above procedure, the expected number of source particles in each batch selected in energy group i is $\langle n_i \rangle = p_i'\, N$, where N is the total number of source particles per batch. The variance associated with $\langle n_i \rangle$ was eliminated by using quota sampling; i.e., at the beginning of each batch $\langle n_i \rangle$ source particles were assigned *a priori* to belong in the ith energy group. (N and p_i' were fixed so that $\langle n_i \rangle$ would be an integral number.)

The influence of the earth's magnetic field can be taken into account by simply selecting E, θ, and ψ in the manner described above and accepting or rejecting the selected coordinates according to the value of the cutoff energy at zenith angle θ and latitude λ. The cutoff energy is given by (e.g., Hopper [1964]; Haffner [1967])

$$E_{c\lambda}(\theta) = mc^2 \left[\sqrt{1 + \left(\frac{Z\, P_{c\lambda}(\theta)}{mc^2} \right)^2} - 1 \right] \; ,$$

where

$$P_{c\lambda}(\theta) = \text{the cutoff rigidity}$$

$$= \frac{4\,P_V}{r^2(1 + \sqrt{1 - \cos^3\lambda\,\cos\theta})^2} \quad ,$$

P_V = the vertical cutoff rigidity

= $14.9 \cos^4 \lambda$ (for dipole field), in units of GV ,

Z, mc^2 = the charge number and rest energy of the particle,

$r = (R_E + h)/R_E$,

R_E = the radius of the earth,

h = the altitude.

In the present calculations, an r of unity was used.

It is of interest to note that the flux spectrum outside the geomagnetic field and the flux spectrum transmitted through the geomagnetic field can be simply related as

$$\phi^*_\lambda(E) = \frac{\phi_o(E)}{2} F_\lambda(E) \quad ,$$

where

$\phi^*_\lambda(E)$ = the omnidirectional (over 2π) flux at energy E and latitude λ transmitted through the geomagnetic field and incident on the earth's atmosphere,

$\phi_o(E)$ = the omnidirectional (over 4π) flux at energy E outside the geomagnetic field,

$F_\lambda(E)$ = the flux transmission factor at energy E and latitude λ.

The expression for $F_\lambda(E)$ can be arrived at by averaging the cutoff energy over all zenith angles; i.e.,

$$\phi^*_\lambda(E) = \int_{4\pi} \phi(E,\bar{\Omega})\ h_\lambda(\theta)\ d\bar{\Omega}$$

$$= \frac{\phi_o(E)}{2} \int_o^{\pi/2} h_\lambda(\theta)\ \sin\theta\ d\theta\ ,$$

where

$$h_\lambda(\theta) = 1 \text{ if } E \geq E_{c\lambda}(\theta)\ ,$$

$$= 0, \text{ otherwise.}$$

Thus,

$$F_\lambda(E) = \int_o^{\theta_c} \sin\theta\ d\theta$$

$$= 1 - \sqrt{1 - \sin^2\theta_c}\ \ ,$$

where

$$\theta_c = \text{the angle at which } E = E_c\ \ ,$$

$$\sin^2\theta_c = \frac{\varepsilon(2-\varepsilon)}{\cos^3\lambda}\ \ ,$$

and

$$\varepsilon^2 = \frac{4\ P_v\ Z}{\sqrt{E(E/mc^2 + 1)}}\ \ .$$

Figures A1 and A2 show $\phi^*_\lambda(E)$ at various λ for protons and alpha particles, respectively, and support the statement made in the text that at the latitude of interest here (42°) the transmitted flux spectrum has a sharp energy cutoff.

It is also of interest to consider the latitude dependence of the number of protons and alpha particles transmitted. Figure A3 shows the integral proton flux, $\Phi^*_{\lambda,p}$, the integral alpha-particle flux, $\Phi^*_{\lambda,\alpha}$, and the ratio $R_{\alpha/p} = \Phi^*_{\lambda,\alpha}/\Phi^*_{\lambda,p}$,

where

$$\phi_\lambda^* = \int_{30\ \mathrm{MeV}}^{\infty} \frac{\phi_o(E)}{2} F_\lambda(E)\ dE\ .$$

At the latitude of interest here (42°), $R_{\alpha/p} \approx 0.25$.

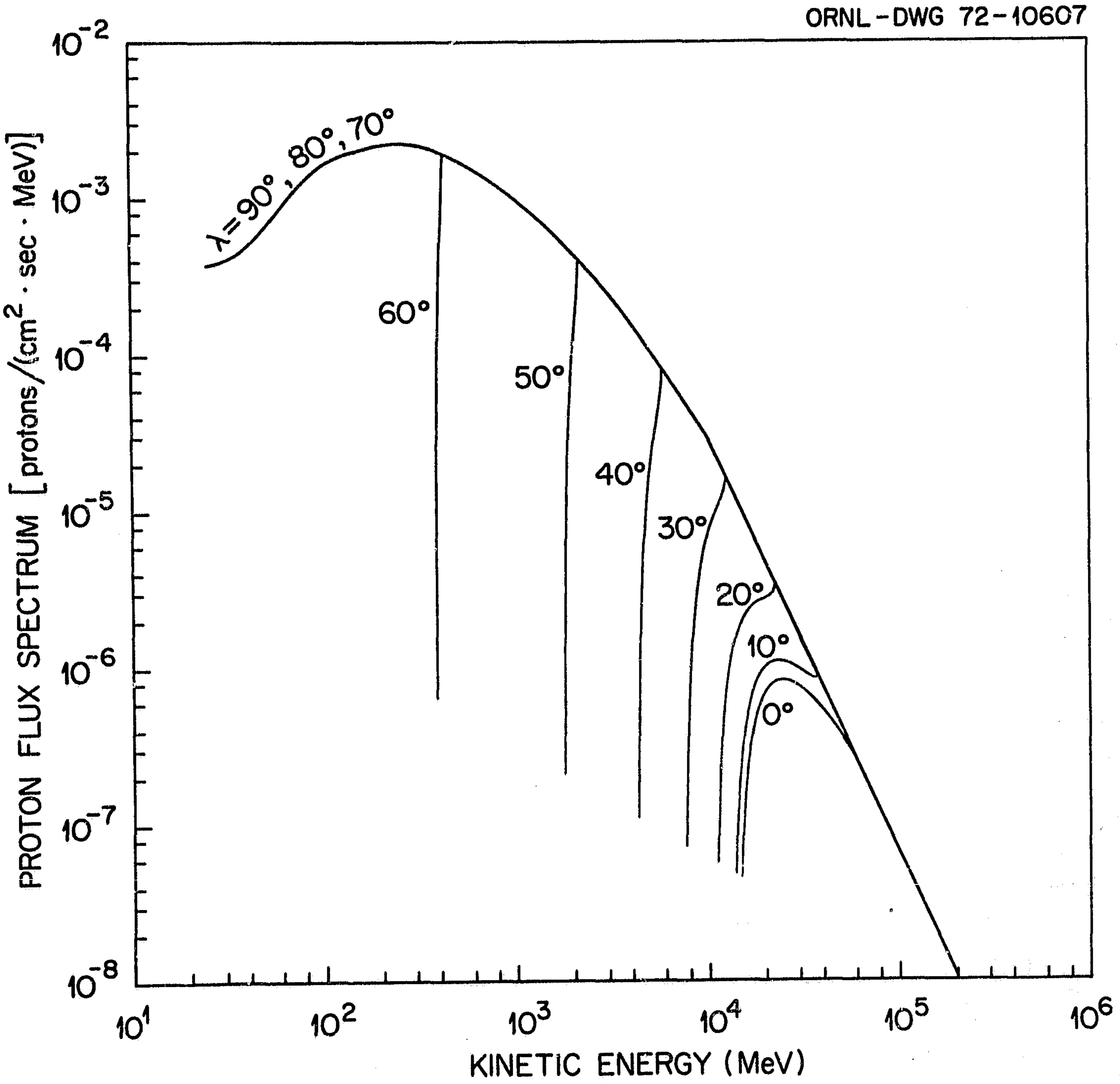

Fig. A1. Solar-minimum proton-flux spectrum at various geomagnetic latitudes.

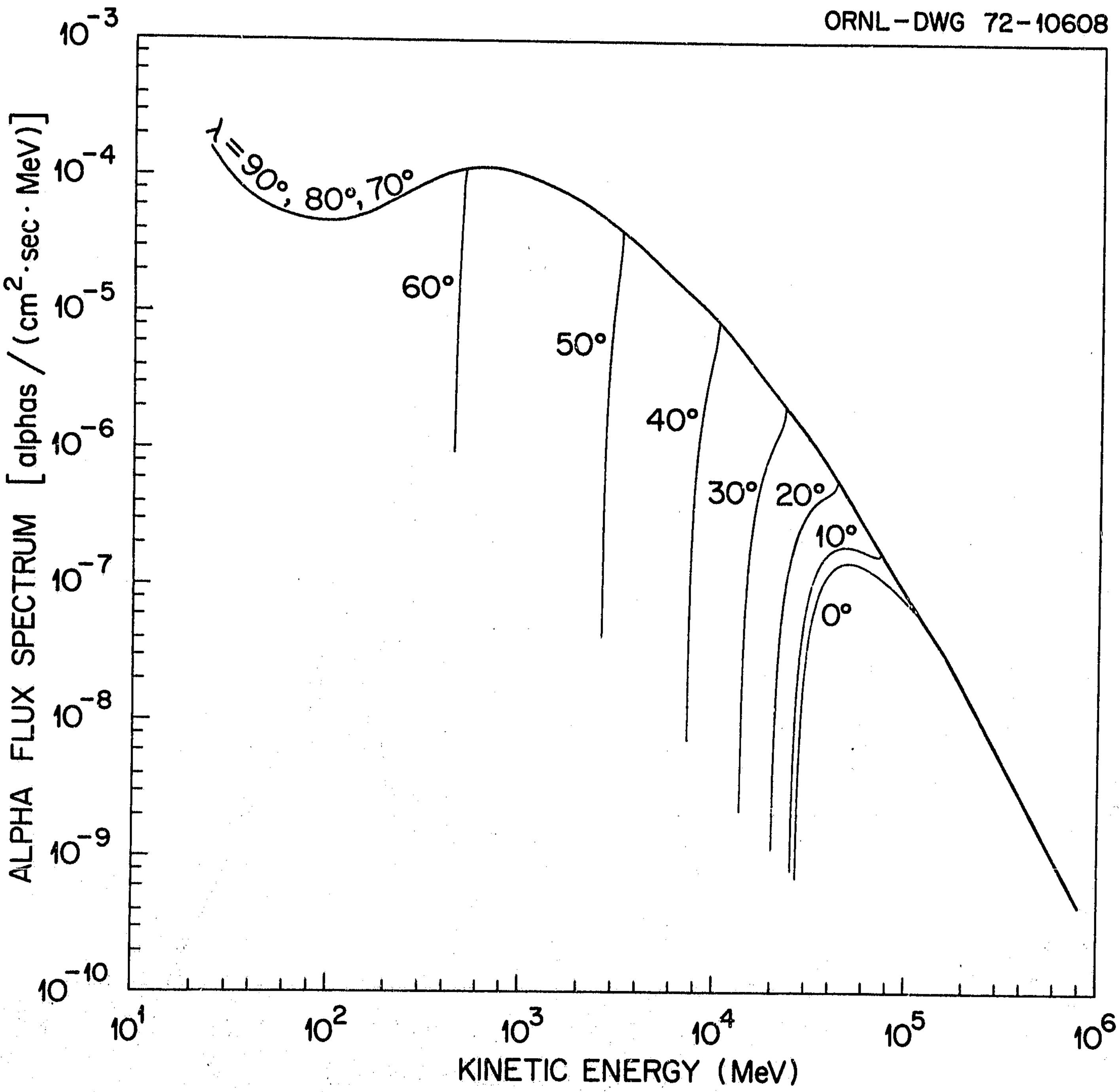

Fig. A2. Solar-minimum alpha-particle-flux spectrum at various geomagnetic latitudes.

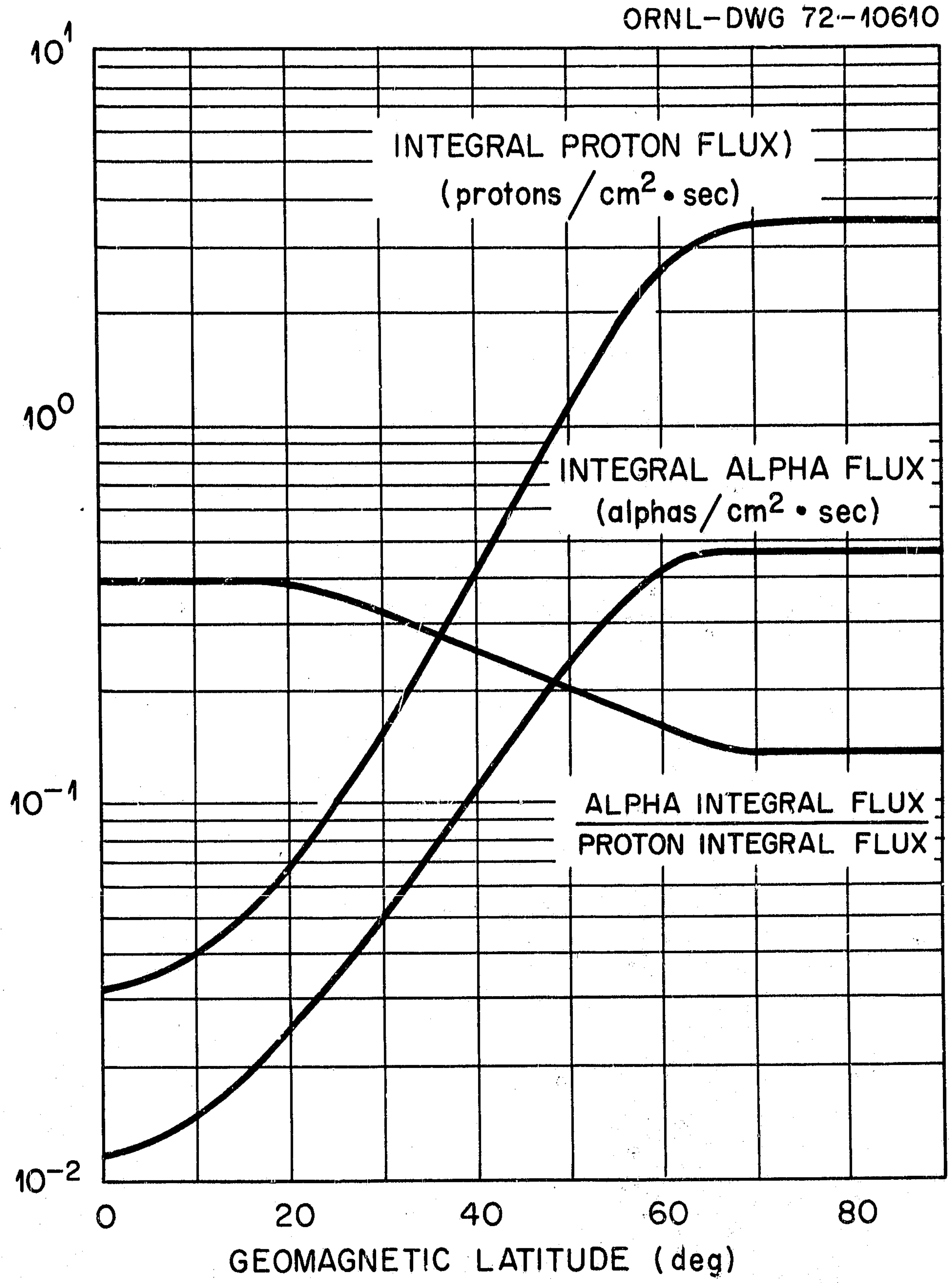

Fig. A3. Integral proton flux, integral alpha-particle flux, and the alpha-particle-to-proton-integral-flux ratio vs geomagnetic latitude at solar minimum.

ACKNOWLEDGMENTS

We wish to thank the following staff members of the Oak Ridge National Laboratory for their assistance: R. G. Alsmiller, Jr. for numerous helpful discussions, W. W. Engle, Jr. for his assistance related to the operation of the ANISN code, and N. M. Greene and J. E. White for their work in obtaining the required low-energy neutron cross-section data.

REFERENCES

Armstrong, T. W., and R. G. Alsmiller, Jr., An approximate density-effect correction for the ionization loss of charged particles, Nucl. Instr. Meth. 82, 289-290, 1970.

Armstrong, T. W., and R. G. Alsmiller, Jr., Calculation of cosmogenic radionuclides in the moon and comparison with Apollo measurements, Proc. Apollo 12 Lunar Science Conf., Geochim. Cosmochim. Acta Vol. 2, Suppl. 2, 1729-1745, M.I.T. Press, 1971.

Armstrong, T. W., R. G. Alsmiller, Jr., K. C. Chandler, and B. L. Bishop, Monte Carlo calculations of high-energy nucleon-meson cascades and comparison with experiment, Nucl. Sci. Eng. 49, 82-92, 1972.

Barkas, Walter H., and Martin J. Berger, Tables of energy losses and ranges of heavy charged particles, NASA SP-3013, 1964.

Beckurts, K. H., and K. Wirtz (translated by L. Dresner), Neutron Physics, (Springer-Verlag, New York, 1964).

Bertini, Hugo W., and Miriam P. Guthrie, Results from medium-energy intranuclear-cascade calculation, Nucl. Phys. A169, 670-672, 1971.

Boella, G., G. Delgli Antoni, C. Dilworth, G. Giannelli, E. Rocca, L. Scarsi, and D. Shapiro, Measurement of the cosmic-ray neutron flux in the atmosphere, Nuovo Cimento Vol. XXIX, N. 1, 103-117, 1963.

Chandler, K. C., and T. W. Armstrong, Operating instructions for the high-energy nucleon-meson transport code HETC, ORNL-4744, Oak Ridge National Laboratory, 1972.

Dragt, Alex J., Michael M. Austin, and R. Stephen White, Cosmic ray and solar proton albedo neutron decay injection, J. Geophys. Res. 71, 1293-1304, 1966.

ENDF/B, Version III, Ed., M. K. Drake, Data formats and procedure for the ENDF neutron cross section library, BNL-50279, Brookhaven National Laboratory, 1970.

Engle, W. W., Jr., A users manual for ANISN, a one-dimensional discrete ordinates transport code with anisotropic scattering, K-1693, Computing Technology Center, Union Carbide Corporation, 1967.

Farley, T. A., A. D. Tomassian, and Martin Walt, Source of high-energy protons in the Van Allen radiation belt, Phys. Rev. Letters 25, 47-49, 1970.

Filz, R. C., and E. Holeman, Time and altitude dependence of 55-MeV trapped protons, August 1961 to June 1964, J. Geophys. Res. 70, 5807-5822, 1965.

Freden, Stanley C., and R. Stephen White, Trapped proton and cosmic-ray albedo neutron fluxes, J. Geophys. Res. 67, 25-29, 1962.

Gabriel, T. A., R. G. Alsmiller, Jr., and M. P. Guthrie, An extrapolation method for predicting nucleon and pion differential production cross sections from high-energy (> 3 GeV) nucleon-nucleus collisions, ORNL-4542, Oak Ridge National Laboratory, 1970.

Gabriel, T. A., R. T. Santoro, and R. G. Alsmiller, Jr., An approximate high-energy alpha-particle-nucleus-collision model, Nucl. Sci. Eng. 44, 104-110, 1971.

Greene, N. M., J. L. Lucius, J. E. White, R. Q. Wright, C. W. Craven, Jr., and M. L. Tobias, XLACS: a program to produce weighted multigroup neutron cross sections from ENDF/B, ORNL-TM-3646, Oak Ridge National Laboratory, 1972.

Haffner, J. W., Radiation and Shielding in Space (Academic Press, New York and London, 1967), p. 287.

Haymes, Robert C., Fast neutron flux in the earth's atmosphere, J. Geophys. Res. 69, 841-852, 1964.

Hess, Wilmot N., H. Wade Patterson, Roger Wallace, and Edward L. Chupp, Cosmic-ray neutron energy spectrum, Phys. Rev. 116, 445-457, 1959.

Hess, W. N., E. H. Canfield, and R. E. Lingenfelter, Cosmic-ray neutron demography, J. Geophys. Res. 66, 665-677, 1961.

Hess, W. N., and John Killeen, Spatial distribution of protons from neutron decay trapped by the geomagnetic field, J. Geophys. Res. 71, 2799-2810, 1966.

Holt, S. S., R. B. Mendell, and S. A. Korff, Fast neutron latitude variations in the atmosphere at solar minimum, J. Geophys. Res. 71, 5109-5116, 1966.

Hopper, V. D., Cosmic Radiation and High Energy Interactions (Prentice-Hall, Inc., Englewood Cliffs, N. J., 1964), p. 133.

Leavitt, C. P., University of New Mexico, private communication, 1972.

Lingenfelter, R. E., The cosmic-ray neutron leakage flux, J. Geophys. Res. 68, 5633-5639, 1963.

Lingenfelter, R. E., Institute of Geophysics & Planetary Physics, UCLA, private communication, 1972.

McDonald, F. B., IQSY observations of low-energy galactic and solar cosmic rays, in Annals of the IQSY, Vol. 4, edited by A. C. Strickland (The M.I.T. Press, Cambridge, 1969), pp. 187-216.

Merker, M., E. S. Light, R. B. Mendell, and S. A. Korff, The flux of fast neutrons in the atmosphere, Proc. 11th Intl. Conf. on Cosmic Rays, Budapest, 1969, Acta Physica Academiae Scientiarium Hungaricae 29, Suppl. 2, 739-744, 1970.

Newkirk, L. L., Calculation of low-energy neutron flux in the atmosphere by the S_n method, J. Geophys. Res. 68, 1825-1833, 1963.

O'Brien, K., Cosmic-ray propagation in the atmosphere, Nuovo Cimento Vol. 3A, N.3, 521-547, 1971.

Preszler, Alan M., George M. Simnett, and R. Stephen White, Earth albedo neutrons from 10 to 100 MeV, Phys. Rev. Letters 28, No. 15, 982-985, 1972.

Singer, S. F., Trapped albedo theory of the radiation belt, Phys. Rev. Letters 1, 181, 1958.

U.S. Standard Atmosphere, 1962, U.S. Government Printing Office, Washington, D. C., 1962.

Webber, W. R., The spectrum and charge composition of the primary cosmic radiation, in Encylopedia of Physics, edited by S. Flugge, Vol. XLVI/2, Cosmic Rays, II, edited by K. Sitte (Springer-Verlag, 1967), pp. 209-264.

White, R. S., S. Moon, A. M. Preszler, and G. M. Simnett, Earth albedo and solar neutrons, IGPP-UCR-72-16, University of California, Riverside, 1972.

Yamashita, Mikio, Lloyd D. Stephens, and H. Wade Patterson, Cosmic-ray-produced neutrons at ground level: neutron production rate and flux distribution, J. Geophys. Res. 71, No. 16, 3817-3834, 1966.

Zobel, W., T. A. Love, J. T. Delorenzo, C. O. McNew, R. H. Baldry, and H. W. Parker, Neutron spectral measurements in the upper atmosphere, ORNL-TM-3877, Oak Ridge National Laboratory, to be published.

END

DATE FILMED

12/ 13 / 72